# Research Aircraft Determination of D-Value Cross Sections

THOMAS R. PARISH

*Department of Atmospheric Science, University of Wyoming, Laramie, Wyoming*

DAVID A. RAHN

*Department of Geography and Atmospheric Science, University of Kansas, Lawrence, Kansas*

DAVE LEON

*Department of Atmospheric Science, University of Wyoming, Laramie, Wyoming*

(Manuscript received 28 August 2015, in final form 24 November 2015)

ABSTRACT

Use of an airborne platform to determine the dynamics of atmospheric motion has been ongoing for over three decades. Much of the effort has been centered on the determination of the horizontal pressure gradient force along an isobaric surface, and with wind measurements the nongeostrophic components of motion can be obtained. Recent advances using differential GPS-based altitude measurements allow accurate assessment of the geostrophic wind. Porpoise or sawtooth maneuvers are used to determine the vertical cross section of the horizontal pressure gradient force. D-values, the difference of the height of a given pressure level from that in a reference atmosphere, are used to isolate the vertical structure of the horizontal component of the pressure gradient force from the vastly larger hydrostatic pressure gradient. Comparison of measured D-value cross sections with airborne measurements of the horizontal pressure gradient is shown. Comparison of D-values with output from the WRF Model demonstrates that the airborne measurements are consistent with finescale numerical simulations. This technique provides a means of inferring the thermal wind, thereby enabling a detailed examination of the vertical structure of the forcing of mesoscale and synoptic-scale wind regimes.

## 1. Introduction

D-values were introduced by Bellamy (1945). D-values are simply the difference between the height of a particular pressure surface above sea level and the height of that same isobaric surface from the U.S. Standard Atmosphere. Bellamy (1945) pointed out that the horizontal pressure gradient force (PGF) is proportional to the variation of D-values along an isobaric surface, and thus D-values are a convenient parameter to describe the vertical structure of the atmosphere. D-values were subsequently used in aircraft studies of jet streak dynamics (Shapiro and Kennedy 1981; Brown et al. 1981) and cloud perturbation pressures (LeMone and Tarleton 1986; LeMone et al. 1988). Recent work with research aircraft

that employ differential GPS processing to permit precise determination of the vertical position (e.g., Parish et al. 2007; Parish and Leon 2013) now enable D-values to be determined with a high degree of precision.

As noted by Bellamy (1945), D-values facilitate visualization of the vertical structure of pressure systems in atmospheric cross sections. When combined with temperature measurements, the influence of the thermal wind on vertical changes in the PGF can be graphically displayed. Although height and D-value variations along an isobaric surface are each proportional to the geostrophic wind, depiction of the PGF in cross sections is difficult without removal of the mean height field. Consider that the PGF, as represented as isobaric changes in height, typically corresponds to differences on the order of 10 m over a 100-km horizontal length scale ($10^{-4}$). Such changes are overwhelmed by hydrostatic pressure gradients which, by definition, are very close to unity. Use of D-values effectively removes the hydrostatic component of the pressure change, so that
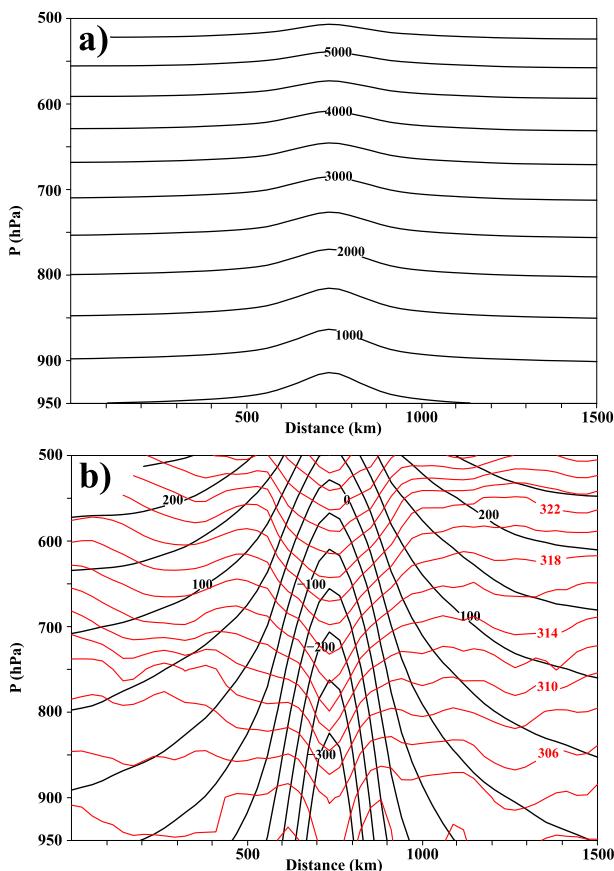
FIG. 1. Cross section from WRF simulation of Hurricane Katrina through the center of the storm at 1200 UTC 28 Aug 2005 showing (a) height of isobaric surfaces (black lines, m) and (b) D-values (black lines, m) and temperature (red lines, K).

horizontal forcing mechanisms can be revealed in detail on atmospheric cross sections (e.g., Fig. 13 in Bellamy 1945).

As an example, consider the finescale height fields associated with the mature stage of Hurricane Katrina. This case study is an example in the Advanced Research version of the Weather Research and Forecasting (ARW; Skamarock et al. 2008) online tutorial used to introduce users to the WRF Model (http://www2.mmm.ucar.edu/wrf/OnLineTutorial). Results are shown after a 12-h simulation using a single domain with 30-km grid spacing. Figure 1 shows zonal cross sections through the eye of the hurricane. Isobaric heights as a function of pressure from near the surface to 500 hPa are shown in Fig. 1a. It is readily apparent that the (low) isobaric height anomaly decreases with height. Even in this extreme case, isobaric heights reveal only general trends within the vertical structure of the PGF. In contrast, Fig. 1b shows the D-values associated with the hurricane. The structure of the hurricane is revealed in more detail, making it possible to

estimate the PGF at any level and rendering vertical changes in the PGF readily apparent.

The isobaric temperature gradient defines the thermal wind, which in turn dictates the vertical change of the PGF and hence the change of the geostrophic wind in the direction normal to the cross section. Temperatures, shown in Fig. 1b, clearly depict the warm-core nature of this low pressure system. As with any warm-core cyclonic feature, the thermal wind opposes the primary circulation of the hurricane and the PGF decreases with height. It is apparent in Fig. 1b that the temperature field is related to vertical changes in the isobaric D-value gradient. Although Fig. 1b illustrates the cross section of temperature, potential temperatures could be used as well since isotherms on an isobaric map are also isentropes, and thus the isobaric gradients of temperature are identical to isobaric gradients of potential temperature.

The purpose of this paper is to demonstrate the ability of research aircraft to infer high-fidelity D-values analyses from common vertical sawtooth flight maneuvers. The resulting D-value cross sections are shown to be internally consistent with the thermal wind and hence the isobaric temperature field. Aircraft measurements are compared with direct measurements of the PGF from isobaric flight legs to show the validity of the D-value analysis and are consistent with results from finescale numerical simulations.

## 2. Determination of D-values using research aircraft

D-value analyses are computed from the dataset collected during the Precision Atmospheric Marine Boundary Layer Experiment (PreAMBLE), a field study conducted from mid-May to mid-June 2012 based in Southern California. The primary goal of PreAMBLE was to study the atmospheric dynamics of the marine boundary layer (MBL) near Point Conception and in particular the pronounced changes of the wind and pressure field associated with topographic features. The impact of such topographic features on the MBL has been convincingly made by Dorman and Koračin (2008).

Airborne determination of D-values requires two measurements: aircraft altitude above sea level and static pressure. Determination of aircraft altitude is achieved by differential GPS processing. Two GPS receivers, an Ashtech Z-Sensor and a Trimble NetRS, are part of the University of Wyoming King Air (UWKA) instrumentation package. Postprocessing software enables the vertical position of the aircraft to be resolved to decimeters (e.g., Parish et al. 2007; Parish and Leon 2013).

Parish and Leon (2013) concluded that the static pressure measurement, rather than aircraft altitude, is

now the limiting factor. The static pressure measurement and correction process is examined in Rodi and Leon (2012). These corrections have been applied to the static pressure values used in this study. To correct for small biases in static pressure during ascents and descents, a linear regression of static pressure to aircraft pitch was employed as was a correction for changes in the altitude of the receiver antenna due to changes in pitch. In the Rodi and Leon (2012) study, typical errors in static pressure of 0.1 hPa were noted. In terms of D-values, such an uncertainty amounts to approximately a 1-m height.

As noted in Bellamy (1945), the PGF can be expressed in terms of the D-value as

$$F_P = -g\left(\frac{\partial D}{\partial n}\right)_P,$$

where $F_P$ is the horizontal component of the pressure gradient force along an isobaric surface, $g$ is the acceleration due to gravity, and the D-value gradient is taken along an isobaric surface with a distance component in the plane of the cross section $n$. Strictly speaking, the PGF along a constant height surface is expressed as

$$F_H = -g(1 + S^*)\left(\frac{\partial D}{\partial n}\right)_H,$$

where $F_H$ is the horizontal component of the pressure gradient force along a constant height surface and the gradient is now taken along the constant height surface. The specific virtual temperature anomaly $S^*$ is defined as

$$S^* = \frac{T^* - T_P}{T_P},$$

where $T^*$ is the virtual temperature and $T_P$ is the U.S. Standard Atmosphere temperature at a given pressure. In a practical sense, $S^*$ is almost always less than about 0.05, and hence variation of D-values along a horizontal surface is approximately the same as variation of D-values along an isobaric surface.

To create a cross section of D-values, a flight must incorporate a series of vertical porpoise or sawtooth maneuvers. Such flight patterns are commonly used to enable the determination of the overall kinematic and thermodynamic structure of the atmosphere. During PreAMBLE, numerous vertical sawtooth legs were conducted. As an example, Fig. 2 shows results from a flight leg conducted on 19 May 2012 along a track crossing south of Point Conception (Fig. 2a). A vertical sawtooth maneuver was made along this track from which D-values have been calculated (Fig. 2b).

D-values in Fig. 2b show a pronounced horizontal deviation along the lowest levels with the lowest D-values
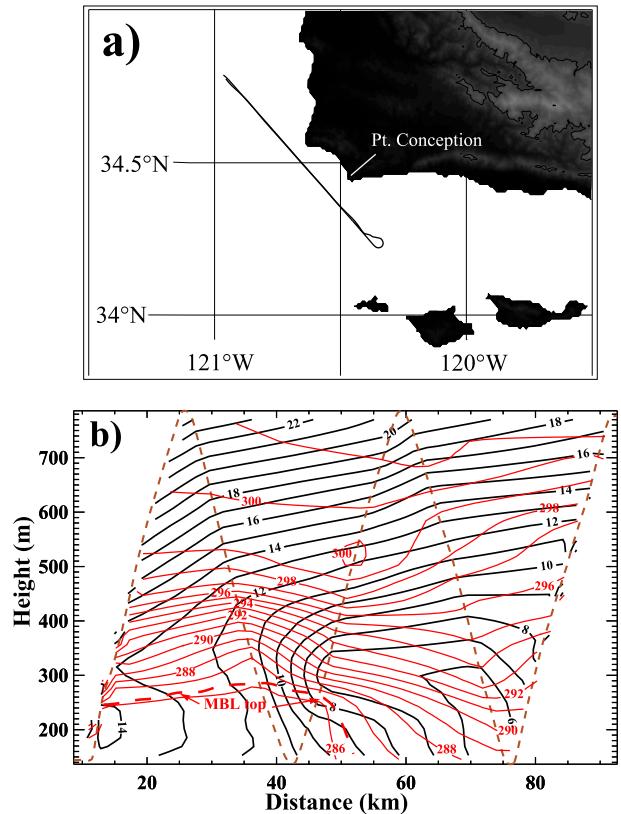


FIG. 2. (a) Track of UWKA from 2011 to 2043 UTC 19 May 2012. (b) Cross-section analysis from aircraft data of D-values (black lines, m) and potential temperature (red lines, K). UWKA track indicated by brown dashed lines; MBL top by red dashed lines. Northwest portion of the track is to the left.

to the right, implying that the PGF is directed from northwest to southeast along the flight track shown in Fig. 2a. The PGF is enhanced midway along the cross section (distances from 40 to 70 km in Fig. 2b), corresponding to the collapse of the MBL south of Point Conception (Rahn et al. 2013). The strongest PGF as evidenced from the D-values analysis is observed at approximately 300 m above sea level near the top of the MBL. The intensity of the PGF decreases rapidly with height.

Strong coupling between the temperature field and D-values is evident in the lower levels of Fig. 2b and provides compelling evidence as to the validity of the D-value analysis. Potential temperatures and D-values are determined independently, yet are intimately related through the thermal wind. Tight vertical packing of isentropes demarcates the inversion capping the MBL that typically marks the location of the strongest PGF. Pronounced vertical changes in the PGF correspond to zones of strong horizontal temperature contrast. Sloping isentropes indicate the presence of the thermal wind; large vertical changes in the D-value
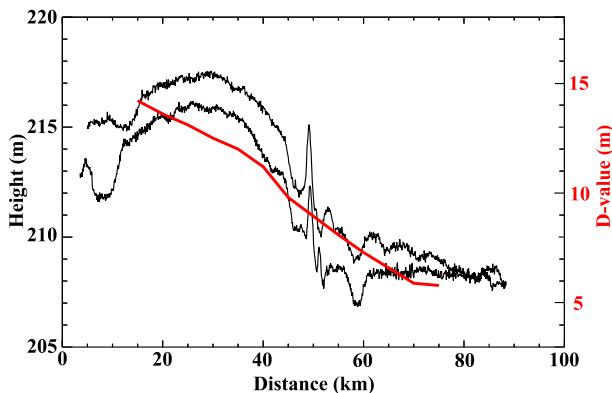
FIG. 3. Heights from the 989-hPa level from measurements taken by UWKA from 1934 to 2009 UTC 19 May 2012 along the same track as shown in Fig. 2a (black lines, m); inferred isobaric heights at the same isobaric level obtained from analysis of D-values from subsequent vertical sawtooth leg from 2011 to 2043 UTC (red line, m). Northwest portion of track is to the left.

gradient between 300 and 400 m occur in response to the thermal wind.

Observations from two isobaric legs conducted along the same track roughly 30 min prior to the sawtooth maneuver are shown in Fig. 3 with D-values from Fig. 2b superimposed. Such legs were conducted frequently during PreAMBLE to directly measure the PGF along key locations. Figure 3 shows the isobaric heights of the 989-hPa surface, roughly corresponding to the 210-m level shown in Fig. 2b. Strong height variations are present along the isobaric surface, again associated with the collapse of the MBL (Rahn et al. 2013). The steep slope of the D-value curve matches heights determined on the previous isobaric legs.

A second example is from the 9 June 2012 case of a Catalina eddy circulation in the California Bight (Parish et al. 2013). This case is noteworthy in that pressure gradients normal to the California coastline are weak, thus making detection of the PGF challenging. This case also featured flight tracks in which reciprocal isobaric legs were followed by vertical sawtooth legs along the same track. This track is shown in Fig. 4a.

D-values from the sawtooth legs are shown in Fig. 4b. In this case, the UWKA porpoised along the track from northeast to southwest and then turned and repeated the maneuver along the track such that the ascent and descent legs were reversed. The D-values show a weak but fairly uniform field, with values increasing slightly along the track in a northeast direction (toward the coast) by 3–4 m comparable to a horizontal pressure increase of 0.2–0.25 hPa.

Although the D-value gradients in the lowest 600–800 m are weak, strong coupling between the temperature and the D-value fields is evident. The MBL for this case slopes upward toward the coast by roughly 100 m. This MBL
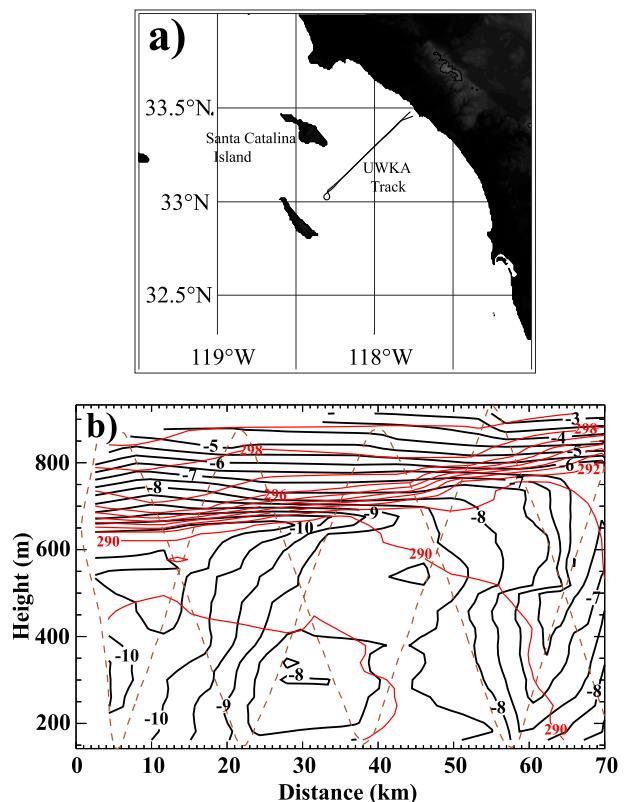


FIG. 4. (a) Track of UWKA in the California Bight from 1526 to 1557 UTC 9 Jun 2012. (b) Cross-section analysis from aircraft data of D-values (black lines, m) and potential temperature (red lines, K). UWKA track indicated by brown dashed lines; southwest is to the left.

slope is responsible for a temperature gradient of roughly 6°C per 50 km. Between 960 hPa and 940 hPa, an $8\,\mathrm{m\,s^{-1}}$ thermal wind results. This implies that that D-value gradient over that same 50 km should decrease by about 4 m over that same vertical distance, in agreement with the observed values.

Isobaric legs, conducted about 30 min prior to the sawtooth legs, were flown at 994 hPa (about 150 m MSL), near the lowest level of the D-value field shown in Fig. 4b and are shown in Fig. 5. Heights slope slightly upward toward the coast with a PGF equivalent to a geostrophic wind component of about $2.8\,\mathrm{m\,s^{-1}}$. Interpolated D-values from the analysis shown in Fig. 4b are superimposed and show the same general trend but with a slightly steeper slope, corresponding to an equivalent geostrophic wind of $3.5\,\mathrm{m\,s^{-1}}$.

## 3. Comparison of D-values with WRF output for the 24 May 2012 PreAMBLE case

D-value fields derived from aircraft measurements also provide a demanding test for numerical models.
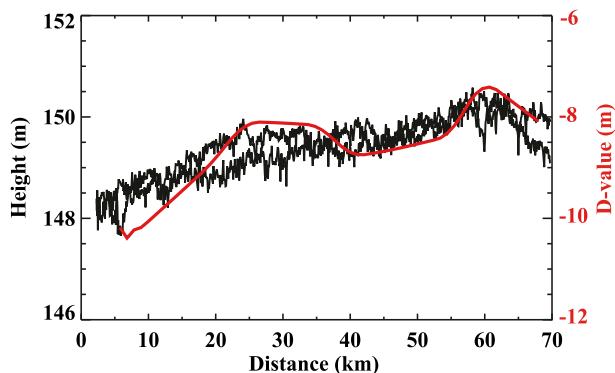
FIG. 5. Heights from the 994-hPa level from measurements taken by UWKA from 1457 to 1526 UTC 9 Jun 2012 along the same track as shown in Fig. 4a (black lines, m); inferred isobaric heights at the same isobaric level obtained from analysis of D-values from subsequent vertical sawtooth leg from 1527 to 1557 UTC (red line, m).

The strongest boundary layer wind speeds during PreAMBLE were experienced on 24 May 2012. A mission was conducted to sample the adjustment of the MBL wind and temperature fields associated with the Point Conception topography. Flight tracks included a sawtooth maneuver along the track shown in Fig. 2a. Given the strong winds in this particular case and previous results (e.g., Koračin and Dorman 2001; Dorman and Koračin 2008; Rahn et al. 2014; Parish et al. 2014), significant modulation of the isobaric height field by the coastal terrain was expected along this track.

To simulate this case, the WRF Model, version 3.5.1, was used with four domains centered just north of Point Conception at a horizontal grid spacing of 27, 9, 3, and 1 km. Each domain consists of 84 sigma levels with increasing resolution toward the surface. Parameterizations used for the run include the Goddard scheme for longwave radiation physics, the Dudhia shortwave radiation scheme, MM5 surface layer similarity with the unified Noah land surface model, and the Yonsei University boundary layer physics scheme. This set of schemes has been shown to reproduce results from the UWKA observations for a number of PreAMBLE cases. The simulation was conducted for the 24-h period commencing at 0000 UTC 24 May 2012. Analysis grids from the 12-km North American Model in 6-h increments were used to initialize the WRF Model. D-values were added to the standard WRF Model output.

D-values from the WRF simulation at 1500 UTC across the track shown in Fig. 2a are depicted in Fig. 6a. The MBL depth is nearly uniform to the northwest of Point Conception but decreases in thickness southeast of the point. D-values suggest a relatively strong PGF.
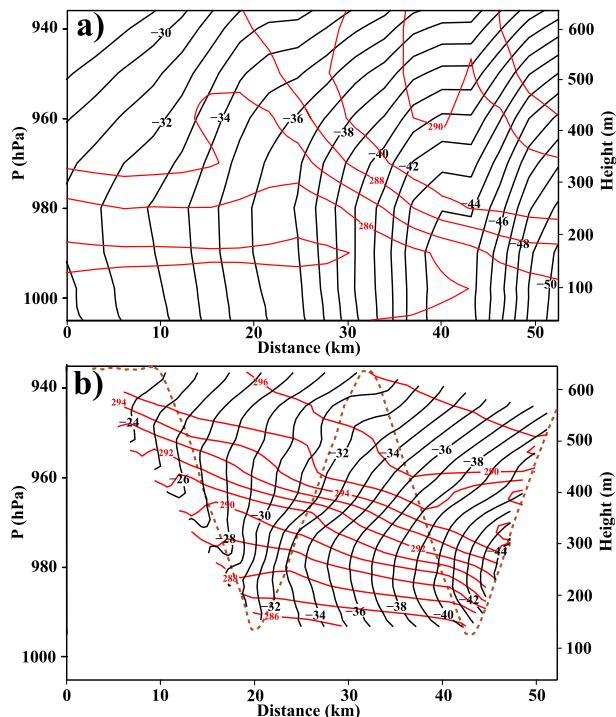


FIG. 6. (a) Results from WRF simulation at 1500 UTC 24 May 2012 showing D-values (black solid lines, m) and potential temperature (red solid line, K) along track similar to that shown in Fig. 2a. (b) Analysis of D-values (black lines, m) and potential temperature (red lines, K) from UWKA sawtooth leg from 1442 to 1455 UTC. UWKA track indicated by brown dashed lines; northwest is to the left.

Within the lowest 200 m of the MBL over the northwest half of the leg, the PGF along the track is directed to the southeast and remains roughly constant with height, consistent with the lack of a horizontal temperature gradient. The low-level PGF is generally stronger in the southeastern half of the leg, and the PGF weakens with height since the thermal wind (directed into the page) opposes the normal component of the geostrophic wind (directed out of the page) as a result of the sloping MBL. Model fields of D-values and temperatures are dynamically consistent through the thermal wind and thus provide a general picture of how the horizontal pressure gradient is influenced by isobaric temperature gradients. UWKA fields of D-values and potential temperature (Fig. 6b) are measured independently. That the D-value field determined from the UWKA sawtooth leg (Fig. 6b) is consistent with the WRF simulation is an indication of the robust nature of the measurement technique. Comparison between UWKA observations and WRF simulations also provides details on the accuracy of the numerical simulation in reproducing details of the MBL adjustment to the local topography along the California coast.

## 4. Summary

Airborne measurement of atmospheric dynamics has been enhanced during the past decade through the advent of differential GPS-based altitudes. These allow for reliable determination of heights along an isobaric surface. Here we have demonstrated the derivation of D-values from aircraft measurements obtained during vertical sawtooth patterns. D-values are clearly linked to the temperature field, thus providing a direct measure of the vertical profile of the thermal wind. The ability to determine the profile of the PGF from an aircraft constitutes a significant advance in our ability to investigate atmospheric dynamics. In the near future we expect to be able to extend this technique using profiles of temperature and humidity retrieved by Raman lidar. By combining measurements of the PGF from several hundred meters above a feature of interest with the temperature field derived from the Multifunction Airborne Raman Lidar (MARLi), the hypsometric equation can be used to infer isobaric heights or D-values in the vertical plane beneath the aircraft.

### REFERENCES

Bellamy, J. C., 1945: The use of pressure altitude and altimeter corrections in meteorology. *J. Meteor.*, **2**, 1–79, doi:10.1175/1520-0469(1945)002<0001:TUOPAA>2.0.CO;2.

Brown, E. N., M. A. Shapiro, P. J. Kennedy, and C. A. Friehe, 1981: The application of airborne radar altimetry to measurement of height and slope of isobaric surfaces. *J. Appl. Meteor.*, **20**, 1070–1075, doi:10.1175/1520-0450(1981)020<1070:TAOARA>2.0.CO;2.

Dorman, C. E., and D. Koračin, 2008: Response of the summer marine layer flow to an extreme California coastal bend. *Mon. Wea. Rev.*, **136**, 2894–2922, doi:10.1175/2007MWR2336.1.

Koračin, D., and C. E. Dorman, 2001: Marine atmospheric boundary divergence and clouds along California in June 1996. *Mon. Wea. Rev.*, **129**, 2040–2056, doi:10.1175/1520-0493(2001)129<2040:MABLDA>2.0.CO;2.

LeMone, M. A., and L. F. Tarleton, 1986: The use of inertial altitude in the determination of the convective-scale pressure field over land. *J. Atmos. Oceanic Technol.*, **3**, 650–661, doi:10.1175/1520-0426(1986)003<0650:TUOIAI>2.0.CO;2.

——, G. M. Barnes, J. C. Fankhauser, and L. F. Tarleton, 1988: Perturbation pressure fields measured by aircraft around the cloud-base updraft of deep convective clouds. *Mon. Wea. Rev.*, **116**, 313–327, doi:10.1175/1520-0493(1988)116<0313:PPFMBA>2.0.CO;2.

Parish, T. R., and D. Leon, 2013: Measurement of cloud perturbation pressures using an instrumented aircraft. *J. Atmos. Oceanic Technol.*, **30**, 215–229, doi:10.1175/JTECH-D-12-00011.1.

——, M. D. Burkhart, and A. R. Rodi, 2007: Determination of the horizontal pressure gradient force using global positioning system on board an instrumented aircraft. *J. Atmos. Oceanic Technol.*, **24**, 521–528, doi:10.1175/JTECH1986.1.

——, D. A. Rahn, and D. Leon, 2013: Airborne observations of a Catalina eddy. *Mon. Wea. Rev.*, **141**, 3300–3313, doi:10.1175/MWR-D-13-00029.1.

——, ——, and ——, 2014: Aircraft observations of the marine boundary layer adjustment near Point Arguello, California. *J. Appl. Meteor. Climatol.*, **53**, 970–989, doi:10.1175/JAMC-D-13-0164.1.

Rahn, D. A., T. R. Parish, and D. Leon, 2013: Airborne measurements of coastal jet transition around Point Conception, California. *Mon. Wea. Rev.*, **141**, 3827–3839, doi:10.1175/MWR-D-13-00030.1.

——, ——, and ——, 2014: Coastal jet adjustment near Point Conception, California, with opposing wind in the bight. *Mon. Wea. Rev.*, **142**, 1344–1360, doi:10.1175/MWR-D-13-00177.1.

Rodi, A. R., and D. Leon, 2012: Correction of static pressure on a research aircraft in accelerated flight using differential pressure measurements. *Atmos. Meas. Tech.*, **5**, 2569–2579, doi:10.5194/amt-5-2569-2012.

Shapiro, M. A., and P. J. Kennedy, 1981: Research aircraft measurements of jet stream geostrophic and ageostrophic winds. *J. Atmos. Sci.*, **38**, 2642–2652, doi:10.1175/1520-0469(1981)038<2642:RAMOJS>2.0.CO;2.

Skamarock, W. C., and Coauthors, 2008: A description of the Advanced Research WRF version 3. NCAR Tech. Note NCAR/TN-475+STR, 113 pp., doi:10.5065/D68S4MVH.